Colloids and Surfaces A: Physicochem. Eng. Aspects 516 (2017) 72–79

Contents lists available at ScienceDirect

Colloids and Surfaces A: Physicochemical and Engineering Aspects

journal homepage: www.elsevier.com/locate/colsurfa

Kinetic turbidimetry of patchy colloids aggregation: Latex particles immunoagglutination

Alexey A. Polshchitsin[a,c], Vyacheslav M. Nekrasov[a,b], Valentin S. Zakovryashin[c], Galina E. Yakovleva[c], Valeri P. Maltsev[a,b,d], Maxim A. Yurkin[a,b], Andrei V. Chernyshev[a,b,*]

[a] Institute of Chemical Kinetics and Combustion, Institutskaya 3, Novosibirsk 630090, Russia
[b] Novosibirsk State University, Pirogova 2, Novosibirsk 630090, Russia
[c] JSC "VECTOR-BEST", PO BOX 492, Novosibirsk 630117, Russia
[d] Novosibirsk State Medical University, Krasny Prospect 52, Novosibirsk 630091, Russia

HIGHLIGHTS

- A new analytical expression for the treatment of the kinetic turbidimetry of patchy colloids aggregation was derived and verified.
- Diffusion-limited aggregation rate constants of chemically-anisotropic reactants with several small active sites were presented.
- Light scattering cross sections of the aggregates (of fractal structure) were calculated using the superposition T-matrix method.
- Gillespie method was applied to calculate stochastic kinetics of the aggregation (which is essential at low number of active sites on particles).
- A significant effect of the low number of active sites per particle on the turbimetric kinetics was found.

GRAPHICAL ABSTRACT

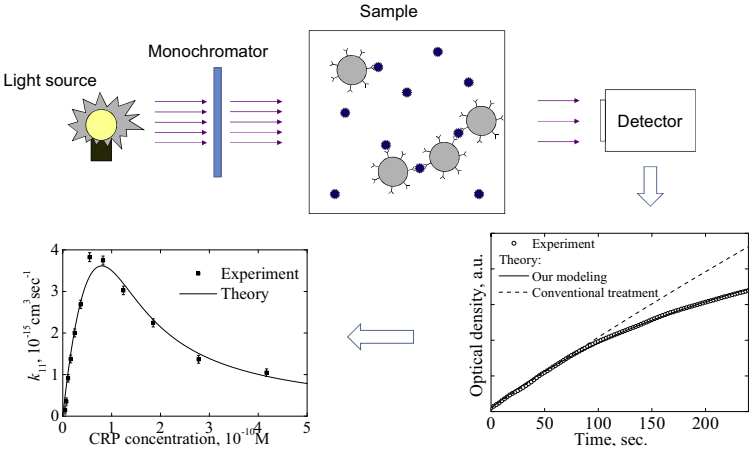

ARTICLE INFO

Article history:
Received 20 October 2016
Received in revised form 9 December 2016
Accepted 10 December 2016
Available online 12 December 2016

Keywords:
Patchy particles
Colloid aggregation kinetics
Latex immunoagglutination
Turbidimetric assay
Fractal clusters
Rate constant
Biospecific binding

ABSTRACT

The paper is devoted to the problem of the kinetic study of aggregation of particles with several active sites (so called "patchy particles") using turbidimetry. Patchy particles are known as chemically-anisotropic reactants, and the kinetics theory of their interaction is far from complete. In this work we theoretically derived and experimentally verified analytical expressions, which are convenient for the treatment of the turbidimetric data on the overall optical density change (due to light scattering of the particles) of the aggregating patchy colloid. Light scattering cross sections of the aggregates were calculated using the superposition T-matrix method. Particularly, we used an analytical approximation for the diffusion-limited rate constants of Smoluchowski equations of aggregation of chemically-anisotropic particles (or clusters) with several small active sites assuming that the clusters are of fractal structure. In order to account for the case of a small (<10) number of active sites on particles we used Monte Carlo stochastic algorithm of Gillespie method. For the verification, we carried out experiments on kinetic turbidimetric study of the immunoagglutination of 65 nm polystyrene particles covered by anti-CRP IgG antibodies in the water solution of C-reactive protein (CRP). Good agreement of experimental data and theoretical

* Corresponding author at: Institute of Chemical Kinetics and Combustion, Institutskaya 3, Novosibirsk 630090, Russia.
E-mail address: chern@ns.kinetics.nsc.ru (A.V. Chernyshev).

http://dx.doi.org/10.1016/j.colsurfa.2016.12.018

Monte-Carlo simulation
Gillespie algorithm

simulations allowed us to evaluate the average number of active antibody molecules per particle as 9.0 ± 2.2 and the affinity of the antigen-antibody complex as $5.5 \pm 1.5 \times 10^7\ M^{-1}$. A significant kinetic effect of the small number of active sites per particle was found.

1. Introduction

Aggregation of particles with several active sites (so called "patchy particles") into branched clusters or into a network with a fixed number of bonding sites has been extensively investigated for the last decades. Fast growing fields of supramolecular chemistry [1,2] and patchy (or "functionalized") colloids [3–5] opened new perspectives in different applications. However, the kinetics of patchy colloids aggregation and self-organization are still largely unexplored [3,6,7]. In the general case of arbitrary number of active sites with arbitrary geometry, modern sophisticated theoretical expressions for the aggregation rate of patchy particles are extremely lengthy and cumbersome (due to chemical anisotropy of the reactants), that is not convenient for treating the experimental data. The aim of the present work is to derive and verify a convenient analytical solution, which gives a simple way of calculating the rate of such sterically specific reaction with high accuracy, and to demonstrate its advantage in the quantification of the patchy colloids aggregation by the optical method.

The most common methods of the colloid aggregation quantification are based on light scattering measurements [8]. And perhaps the most simple and affordable optical equipment is the turbidimetric technique [8–12] that allows one to register the optical density change of a bulk media in the course of the aggregation process with a conventional photometer.

Investigation of aggregation kinetics is generally studied with the use of latex immunoagglutination [13] tests which can act as a simple patchy colloid system. These tests are widely applied in biology and medicine for the determination of antigen or antibody in liquids [14–17]. In immunoagglutination tests, the aggregation of latex particles of micro- or nanometer sizes range is mediated by a biospecific reaction between the antibody and the antigen, one of which ("ligand") is dissolved in the media and the other ("receptor") is immobilized on the particles surface.

1.1. Existing methods of aggregating colloid optical density calculation

Modeling of the colloid optical density change during the aggregation process has been theoretically addressed in the literature [8]. In a relatively low-density colloid, neglecting multiple scattering of light, the overall extinction coefficient α_{ext} is the sum of contributions from individual components [10,15]:

$$\alpha_{ext} = \sum_{i=1}^{\infty} C_i \varepsilon_i \tag{1}$$

where C_i is the concentration of aggregates of i monomers, and ε_i is total light scattering cross sections of corresponding aggregates.

In turbidimetric studies, the radius R_1 of monomer particles is usually from 2 to 10 times smaller than the incident light wavelength λ in order to provide a significant increase of light extinction during the agglutination. In such range of the sizes the Rayleigh theory of light scattering is not applicable. Instead, the Rayleigh-Gans-Debye (RGD) theory and the Mie theory were applied [18–20] to calculate the light scattering cross section of the aggregates in the system. The aggregation rate constants can be estimated from the initial slope [21] of the optical density measured by turbidimetry. Puertas et al. [10] developed a simple model which provides a complete fit of the optical density versus time curve of the coagulation process using the RGD theory and Smoluchowski equations, although the optical properties of growing aggregates exceeded the applicability range of the RGD theory. In contrast to the RGD theory, the Mie theory has no limitations on the particles size and the refractive index, but it can be applied only for spherical particles of uniform internal structure. However, the shape of the aggregate is usually not spherical, and its internal structure is not uniform. A general method for computing light scattering by particles of arbitrary shape and internal structure is the discrete dipole approximation (DDA) [22]. The only limitation of the DDA is the significant computation time.

Recent works revealed that T-matrix method [9,11,20] yields the most rigorous results for monomers and dimers scattering cross sections based on directly solving of Maxwell's equations in a wide range of the size and the refractive index parameters. The comparison of DDA and T-matrix calculations with experimental results shown [23] that both methods provide results with good precision. However, in the case of the aggregates composed from spherical particles, the T-matrix method is more preferable, because it is much faster and has an analytical procedure of the orientation averaging.

In the immunoagglutination model, it is generally assumed that the antigen-antibody binding reaction reaches equilibrium much faster than the aggregation occurs. As a result all monomer particles have equal number of free and bound "receptors" at the very beginning [24]. Then the aggregation is usually considered as an irreversible process described by Smoluchowski equations [3] (if the particles concentration is not very high [25]):

$$\frac{dC_n}{dt} = \frac{1}{2}\sum_{i+j=n} k_{ij} C_i C_j - C_n \sum_{i=1}^{\infty} k_{in} C_i, \tag{2}$$

where k_{ij} is the reaction rate constant between aggregates of i and j particles.

Two distinct classes of aggregation regimes have been investigated. One class is diffusion limited aggregation (DLA) [26,27] which corresponds to a reaction occurring at each encounter between clusters. The well-known formula for the rate constant k_{DLA} of a pure diffusion-controlled binding of two spherical particles is

$$k_{DLA} = 4\pi RDF, \tag{3}$$

where $R = R_1 + R_2$ is the sum of the reactants radii, and $D = D_1 + D_2$ is the sum of the reactants diffusion coefficients, and F is the steric factor. The steric factor F can be sufficiently less 1, if not all surface of the particles are available for binding [28,29].

The other class is reaction limited aggregation (RLA) [30] where the reaction rate k_{RLA} is determined by the probability of forming a bond upon collision of two clusters. In a general case the rate constant k is often [31] expressed by the following approximation

$$k = \left(\frac{1}{k_{DLA}} + \frac{1}{k_{RLA}}\right)^{-1}. \tag{4}$$

Biospecific aggregation, such as immunoagglutination, is a particular case of aggregation. Biologic macromolecules are capable of sterically specific (chemically anisotropic) binding with particular ligands. [32] The reactants can bind to each other only at certain discrete reactive spots (active sites), which are relatively small comparing to the size of reactants. Therefore, one can expect significant steric factor for aggregation kinetics, since specific binding sites occupy a rather small surface fraction of a particle. It is generally believed that the activation energy for the association reaction between ligand and receptor is rather low. Therefore, the reaction rate of biospecific aggregation can be calculated in the diffusion limited regime taking into account a steric factor F, which reduces the DLA rate constant. Standard DLA rate constant is usually expressed by the following equation [33]:

$$k_{ij} = k_{11}\left(i^{1/d} + j^{1/d}\right)\left(i^{-1/d} + j^{-1/d}\right), \tag{5}$$

where d is the aggregates fractal dimension. Surovtsev et al. [34] and Wiklund et al. [35] suggested an extended dependence of k_{ij} on i and j considered clusters as a chemically anisotropic reactants with several active sites on their surface. These extended models interpret experimental data well for the particle with a large number of binding sites. But in the case of submicron particles, which are commonly used as patchy colloids, the aggregation kinetics may be significantly affected by the small number of binding sites. In addition, the relative size of active sites is decreasing, while their number is increasing for growing clusters in the course of the aggregation process. These two aspects are rarely discussed in the literature on patchy colloid aggregation and particularly on immunoagglutination. Recently Nekrasov et al. [36] made an interesting theoretical investigation deriving an analytical formula for k_{ij} in such a more general case, which we apply in this work.

In this work we present a new approach for the modeling of the optical density temporal evolution in the course of the immunoagglutination registered by turbidimetry, which takes into account the discreteness of the binding sites on the particles. The approach is based on Monte Carlo kinetics simulations of the stochastic chemical reactions using Gillespie stochastic algorithm modified for aggregation kinetics. This method allows us to account for the consumption of active sites on the bond formation during aggregation and for the initial distribution of particles over occupied binding sites. The latter feature is crucial in immunoagglutination process modeling at low fractions of occupied reaction sites. Calculation of aggregates optical features was provided with the use of diffusion-limited aggregation method of cluster construction [37]. Light scattering cross sections of the aggregates were calculated using the superposition T-matrix method [38].

2. Theory and simulations

2.1. Sterically specific immunoagglutination

Immunoagglutination assumes two types of active sites on the surface of the particles, – 1) free receptors and 2) receptors occupied by ligand, – and the binding is possible only between free and occupied receptors making receptor-ligand-receptor “bridge” between the two particles. Let the first particle of the radius R_1 has on its surface $N_{x,1}$ free receptors and $N_{y,1}$ occupied receptors, the second particle of the radius R_2 has $N_{x,2}$ and $N_{y,2}$ surface receptors correspondingly. This case for considered in detail in [36], here we briefly repeat those derivations for completeness. In particular, one can use the following approximate expression for the DLA rate constant of the binding (of these two particles) [36]:

$$k = 4\pi(R_1 + R_2)(D_1 + D_2)\left(f_1\sqrt{f_2} + f_2\sqrt{f_1}\right)(N_{x,1}N_{y,2} + N_{y,1}N_{x,2}). \tag{6}$$

where f_1 and f_2 are the surface fractions (steric factors) of a single active site on the first particle and the second particle, correspondingly; D_1 and D_2 are the diffusion coefficients of the particles. It should be noted that Eq. (6) is correct only when the size of the active site (of the receptor) is much less than the distance between the active sites on the particles surface. Eq. (6) reflects the influence of the active sites discreteness on the aggregation rate constant.

In our kinetic model we consider the cluster as a fractal [15,39,40] object of spherical shape. That means the radius $R^{(i)}$ of a cluster consisting of i monomers can be expressed through the monomer radius R, as follows

$$R^{(i)} = Ri^{1/d}, \tag{7}$$

where d is the fractal dimension of the cluster. We assume that the average surface density of all receptors on clusters is not changing during aggregation and the cluster surface available to binding is equal to that of the equivalent sphere. Then the total number $N^{(i)}$ of surface receptors on a cluster of size i:

$$N^{(i)} = Ni^{2/d}. \tag{8}$$

Due to steric complementarity (i.e. biospecificity) of the ligand and the receptor, their corresponding active sites are equal in size (e.g. the effective radius of the spot). Let a be the effective radius of the active site. Then the steric factor $f^{(i)}$ of the active site of the cluster is

$$f^{(i)} = \left(\frac{a}{2R}\right)^2 i^{-2/d}. \tag{9}$$

Diffusion coefficient $D^{(i)}$ of the cluster can be approximated using the Stokes-Einstein formula:

$$D^{(i)} = \frac{k_B T}{6\pi\eta R^{(i)}} = \frac{k_B T i^{-1/d}}{6\pi\eta R}, \tag{10}$$

where η is the viscosity of the media, k_B is the Boltzmann constant, T is the temperature.

If one neglects stochastic variation of the fraction p of occupied surface receptors from particle to particle (due to a finite number of receptors), then each particle (monomer or cluster) has certain number of free $N^{(i)}_{x,n}$ and occupied $N^{(i)}_{y,n}$ receptors on their surface:

$$N^{(i)}_{x,n} = N^{(1)}_x i^{2/d} = (1-p)N^{(1)} i^{2/d}, \tag{11}$$

$$N^{(i)}_{y,n} = N^{(1)}_y i^{2/d} = pN^{(1)} i^{2/d}. \tag{12}$$

Then Eq. (6) leads to the following expression for the binding rate constant k_{ij} between two clusters can be expressed as

$$k_{ij} = \frac{4k_B T}{3\eta}\left(\frac{a}{2R^{(1)}}\right)^3 N^{(1)}_x N^{(1)}_y \left(i^{1/d} + j^{1/d}\right)^2 \left(i^{-1/d} + j^{-1/d}\right). \tag{13}$$

Eq. (13) for the rate constant of Smoluchowski equations (2) can be used to simulate the immunoagglutination kinetics in the case when the number of receptors on the particles surface is large enough to neglect both the loss of the active binding sites during cross linking and the stochastic variation of the fraction of occupied receptors from particle to particle.

In order to simulate the immunoagglutination kinetics in the case of the small number of receptors per particles we build up a “discrete” model of the aggregation, taking into account the finite number of receptors on each particle. This implies stochastic variation of the fraction of occupied receptors from particle to particle described by the binomial distribution:

$$P(N_y; N, p) = \frac{N!}{(N_y)!(N - N_y)!} p^{N_y}(1-p)^{N-N_y}, \tag{14}$$

where $P(N_y; N, p)$ is the probability for the particle with N total surface receptors to have N_y occupied surface receptors if the average fraction of occupied surface receptors is p. This variation is especially important for $Np \sim 1$.

Since ligand molecules diffuse much faster than macroscopic particles, the reaction of ligand molecules with surface receptors reached equilibrium before the aggregation of the particles sufficiently occur. Therefore, the following equation is applied for the average fraction p of occupied surface receptors [34]:

$$p = \frac{1}{2NC_0}(K_d + NC_0 + C_L) - \frac{1}{2NC_0}\sqrt{(K_d + NC_0 + C_L)^2 - 4NC_0C_L}, \tag{15}$$

where C_0 is the initial concentration of monomer particles, K_d is the equilibrium dissociation constant (inverse affinity) of the ligand-receptor complex, C_L is the initial ligand concentration.

We used the following algorithm for the population dynamics simulation. At the beginning of the process all particles are monomers, stochastically distributed over the number of occupied receptors according to Eq. (14). In order to apply Eq. (6) for the simulation one has to know the numbers of free $N_{x,n}^{(i)}$ and occupied $N_{y,n}^{(i)}$ receptors on the reactants (n = 1,2) surface. Due to the fractal structure of the clusters,

$$N_{x,n}^{(i)} = 4\pi R^{(i)2}\frac{X_n^{(i)}}{4\pi R^2 i} = X_n^{(i)} i^{(2/d)-1}, \tag{16}$$

$$N_{y,n}^{(i)} = 4\pi R^{(i)2}\frac{Y_n^{(i)} - (i-1)}{4\pi R^2 i} = \left[Y_n^{(i)} - (i-1)\right] i^{(2/d)-1}, \tag{17}$$

where $Y_n^{(i)}$ and $X_n^{(i)}$ are the total number of ligand molecules and free receptors in the cluster (both on the surface and inside) consisting of i monomers. The term $(i-1)$ in Eq. (17) is the number of bonds between i monomers in the cluster. Taking into account that all monomers have the same total number of surface receptors N, one can calculate $X_n^{(i)}$ through $Y_n^{(i)}$:

$$X_n^{(i)} = iN - Y_n^{(i)} - (i-1). \tag{18}$$

Let us denote the particle number n (monomer or cluster) by the vector $\begin{bmatrix} i \\ Y_n^{(i)} \end{bmatrix}$. Then the reaction scheme can be expressed as

$$\begin{bmatrix} i \\ Y_n^{(i)} \end{bmatrix} + \begin{bmatrix} j \\ Y_m^{(j)} \end{bmatrix} \rightarrow \begin{bmatrix} i+j \\ Y_n^{(i)} + Y_m^{(j)} \end{bmatrix}. \tag{19}$$

The rate constant of the reaction (19) is calculated substituting Eqs. (16)–(18) into Eq. (6).

Thus, the population of particles in the colloid system is represented by the particles concentration $C\left(i, Y_n^{(i)}; t\right)$ as a function of i and $Y_n^{(i)}$ at certain time t. During the aggregation the function $C\left(i, Y_n^{(i)}; t\right)$ is changing according to the reaction scheme (19). Using initial condition based on Eq. (14)

$$C\left(i, Y_n^{(i)}; t = 0\right) = \begin{cases} C_0 P(Y_n^{(1)}; N, p), & i = 1, \\ 0, & i > 1. \end{cases} \tag{20}$$

we calculated the population dynamics $C\left(i, Y_n^{(i)}; t\right)$ using Monte Carlo stochastic simulation algorithm (SSA) of Gillespie [41]. Since the aggregating system is strongly coupled, we chose the direct SSA method [41].

2.2. Light-scattering cross section of the aggregates

We assume that all monomers are spherical particles with the same radius, the refractive index, and the number of receptors on the surface. During irreversible aggregation the particles stick together forming non-spherical clusters of non-uniform internal structures, which can be considered as fractals [15]. We used DLA algorithm [37] for the aggregate spatial construction. For certain fractal parameters (i.e. d and R_1), an ensemble of 100 theoretical aggregates of random structure was theoretically generated. For each aggregate of the ensemble we computed the orientation averaged light scattering cross section using the superposition T-matrix method [38]. Then the result was averaged over the ensemble. The need of such averaging over the ensemble is well established [42].

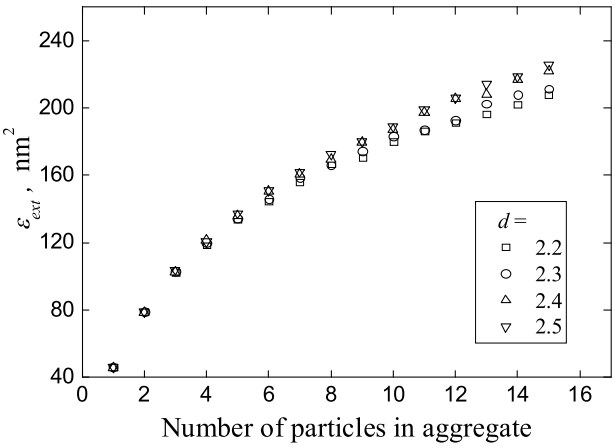

Fig. 1. Extinction cross sections of aggregates with different fractal dimension d.

The light scattering cross sections were calculated assuming the fractal dimension in the range from 2.2 to 2.5, according to experimental data [15]. Refractive indices of particles and media were calculated using known expressions [43] considering our experimental conditions. Fig. 1 shows the calculated cross section of aggregates. We found that the extinction depends insignificantly on d for small aggregates, however, the dependence increases with the number of monomer particles in the cluster. In this work we used the value d = 2.40 for the calculation of the light scattering cross section of aggregates just to work in the middle of experimentally detected range.

3. Materials and methods

In our experiments we decided to use one of the common tests applied in clinical laboratories—the turbidimetric determination of the concentration of C-reactive protein (CRP) with a standard kit (from BioSystems, COD 32321). The concentration of the CRP standard in the kit is traceable to the ERM-DA472/IFCC (Institute for Reference Materials and Measurements, IRMM).

Two reagent solutions were prepared prior to experiments: R1-reagent consisted of entirely the reagent A (Glycine buffer 0.1 mol/L, sodium azide 0.95 g/L, pH 8.6) from the kit; and R2-reagent included the reagent A and the reagent B (suspension of latex particles coated with anti-human CRP antibodies, and sodium azide 0.95 g/L) in a ratio of 4:1. The scheme of the experiment was as follows: 500 μl R1 was mixed with 20 μL solution of different CRP concentrations; then 500 ml R2 was added to the mixture of R1 with CRP and stirred well; then the optical density of the solution was measured for five minutes at 37° C by a spectrophotometer Specord 210 (Analytik Jena, UK) at a wavelength of 540 nm in the plastic disposable cuvette. The range of CRP concentration in reaction volume was from 4.8×10^{-12} to 4.2×10^{-10} mol/L. Antigen solutions were prepared by means of serial dilution of standard sample by the factor 1.5. The optical density of the sample and the blank of the buffer were registered separately for the calculation of the optical density of the microspheres.

The diameter of individual single latex microspheres was determined by the electron microscope JEM 1400 (Jeol, Japan) with

negative staining, and the value 65 ± 2 nm of the average diameter of the particles was obtained.

4. Results and discussion

The kinetics of the immunoagglutination was simulated for certain parameters: the initial concentration of ligand (antigen) dissolved molecules C_L, the ligand-receptor (antigen-antibody) dissociation constant K_d, the initial concentration of particles C_0, the number of "receptors" (antibody molecules) on a single monomer particle N, the radius R and the refractive index of the monomer spherical latex particle. As a result of this simulation, the evolution of the aggregates distribution function $C_i(t)$ was obtained. Concentrations $C_i(t)$ were multiplied by corresponding cross sections ε_i and Eq. (1) was applied to obtain the overall optical density (OD) of the colloid.

In order to simplify and accelerate the treatment of the experimental data, the following analytical approximation of the OD temporal evolution was used (in the form of Pade approximation [44] by a rational function):

$$OD = OD_0 + A\frac{1 + B_1 t}{1 + B_1 B_2 t}, \tag{21}$$

where OD_0 is the optical density of the external media (the buffer), which does not contain particles, A is the optical density of the particles at the very beginning (all particles are monomers), B_1 and B_2 are independent parameters. The first two parameters OD_0 and A are obtained prior to the immunoagglutination procedure and have a well-defined physical meaning. The last two parameters B_1 and B_2 are obtained by non-linear regression of the theoretical OD temporal profile to the experimental one. Using the Pade approximant (21) one has a bijection between the couple of parameters (B_1, B_2) and the target couple of parameters (N, p) that allows the determination of the target protein concentration from the turbidimetric data. The form of function (21) is chosen to make one parameter (B_1) to be implicitly bound with the reaction rate and second parameter (B_2) to be responsible for dissimilarity of OD curves for different antigen concentrations.

As a result of the approximation of OD curves calculated using the Monte-Carlo algorithm, the need to store the explicit form of the optical density kinetics in the database was eliminated. Instead, the database included only parameters B_1 and B_2, which allows one to uniquely recover the curve with corresponding N and p. Maximum errors of parameters B_1 and B_2 determination in fitting were less than 5% with the mean errors equal to 1%. Constructed bijection on the one hand, does not significantly worsen the accuracy of the data interpretation, on the other hand, simplifies the analysis and comparison of the optical density kinetics.

Fig. 2 shows the dependence of B_1 and B_2 on p for different N. Some noise in the presented values seems to be associated with the underlying Monte Carlo algorithm. However, there is a characteristic flattening trend with p approaching 0.5, which is due to the symmetry of the whole problem with respect to the transformation $p \to (1 - p)$. We can see that the dependences of the B_2 parameter change a little for different N for values greater than 25, but for lesser values they are markedly different. Parameters B_1 vary much more and are a major reason of change in the kinetics of the optical density. Such a behavior of B_2 parameter indicates that optical density curves are self-similar for different large enough occupancy fractions p, other things being equal. Therefore, the use of such optical density curve parameterization allows one to evaluate the limits of time-scaling method applicability and shows the extreme necessity of the consideration of the limited number of discrete active sites of single particles.

In Eq. (21) we assumed that there were only monomer particles in the colloid at the very beginning ($t = 0$) of the aggregation.

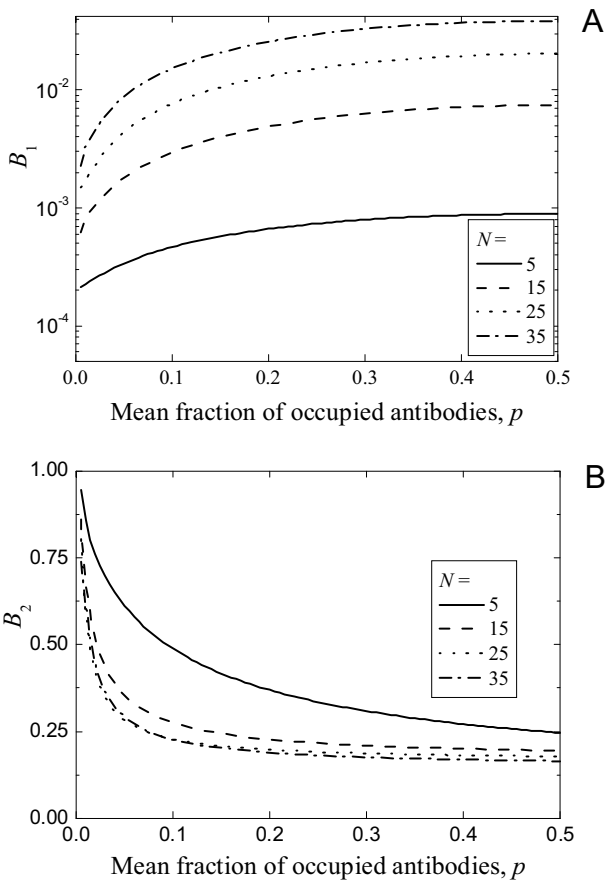

Fig. 2. The dependence of *B1* (A) and *B2* (B) on p for various *N*.

However, in practical applications some fraction of aggregates can exist in the system at the very early stage (for example, due to the acceleration of the aggregation by the mixing procedure during the sample preparation). The effect of these initial aggregates on the OD temporal profile may be significant even when their concentration is relatively low. To take into account the presence of unknown concentration of initial aggregates we suggest using the following modification of the Eq. (21) for the experimental data treatment:

$$OD = OD_0 + A\frac{1 + B'_1 (t + t_0)}{1 + B'_1 B'_2 (t + t_0)}, \tag{22}$$

where t_0 is the "time shift" for the compensation of the OD temporal profile change. In order to investigate the applicability of Eq. (22) we computed the OD temporal profile change in the presence of the initial dimers additive of different initial concentrations (from 0 to 10% of the total concentration of initial particles $C_\Sigma = C_1 + C_2$) and at certain parameters (N, p). We neglect the effect of higher aggregates on the initial optical density, since the concentration of larger aggregates are typically much less than the concentration of dimers at the initial stage of the monomers aggregation [45]. The OD curve was fitted by Eq. (21) at $C_2 = 0$ yielding parameters (B_1, B_2) and by Eq. (22) at $C_2 > 0$ yielding parameters (B'_1, B'_2). Fig. 3 shows that parameters (B_1, B_2) and (B'_1, B'_2) does not significantly differ from each other if the fraction of the initial dimers is less than 10%. Therefore, we further applied Eq. (22) for the treatment of our experimental data.

The new method of the treatment of turbidimetric experimental data was applied for immunoagglutination kinetics measured in 12 samples, which covered the range of CRP concentration from 4.8×10^{-12} to 4.2×10^{-10} mol/L. The registered OD temporal curves were fitted by non-linear regression with Eq. (22) (see Fig. 4) to

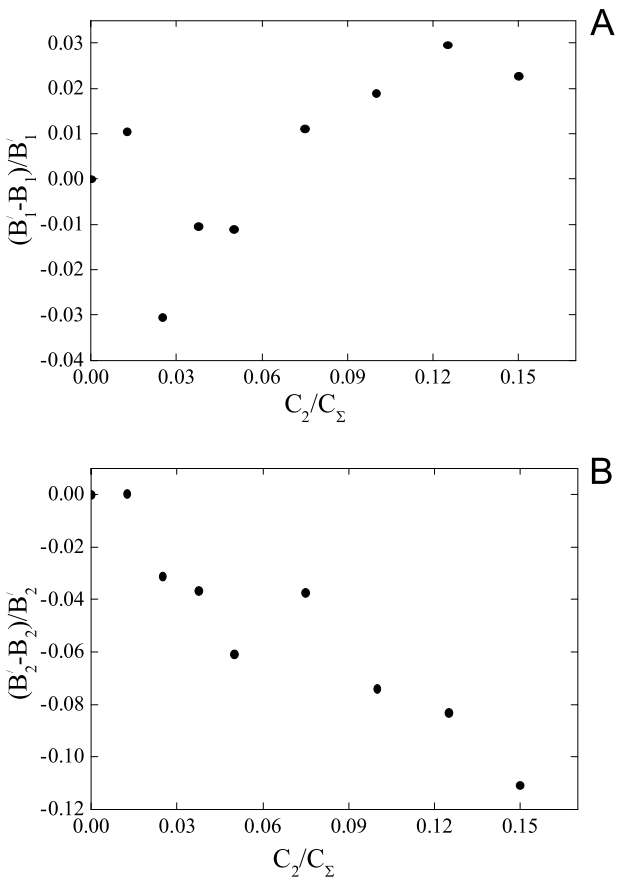

Fig. 3. The relative variation of parameters *B1* (A) and *B2* (B) in Eq. (22) if a portion of particles are in state of dimers with the concentration C*2* (the total concentration C_Σ).

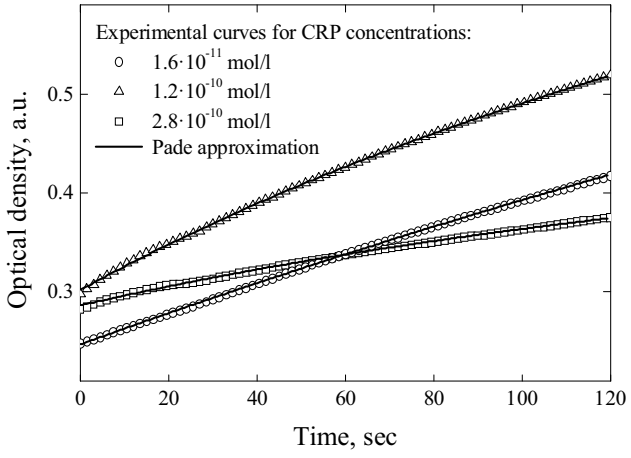

Fig. 4. Experimental OD temporal curves fitted by Eq. (22).

find the parameters (B_1,B_2), which are determined by the target CRP concentration. The necessity of the compensation parameter t_0 of Eq. (22) for this treatment is demonstrated in Fig. 5 for various initial concentration of the ligand (antigen). The values lie in a narrow range in the region of free surface antibodies predominance. But in the region of occupied surface antibodies predominance one can see an increase of t_0 value with the concentration of CRP and a tendency to saturation. This behavior is a result of system passage through the different fractions of occupied surface antibodies, including the most effective for agglutination value $p = 0.5$, with permanently reacting particles during a mixing procedure.

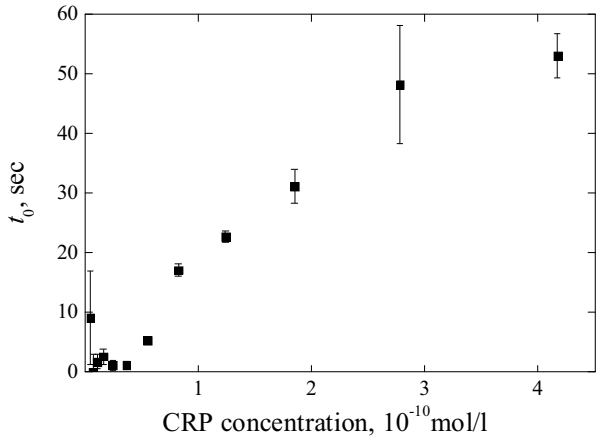

Fig. 5. Shift time *t0* for various CRP concentrations.

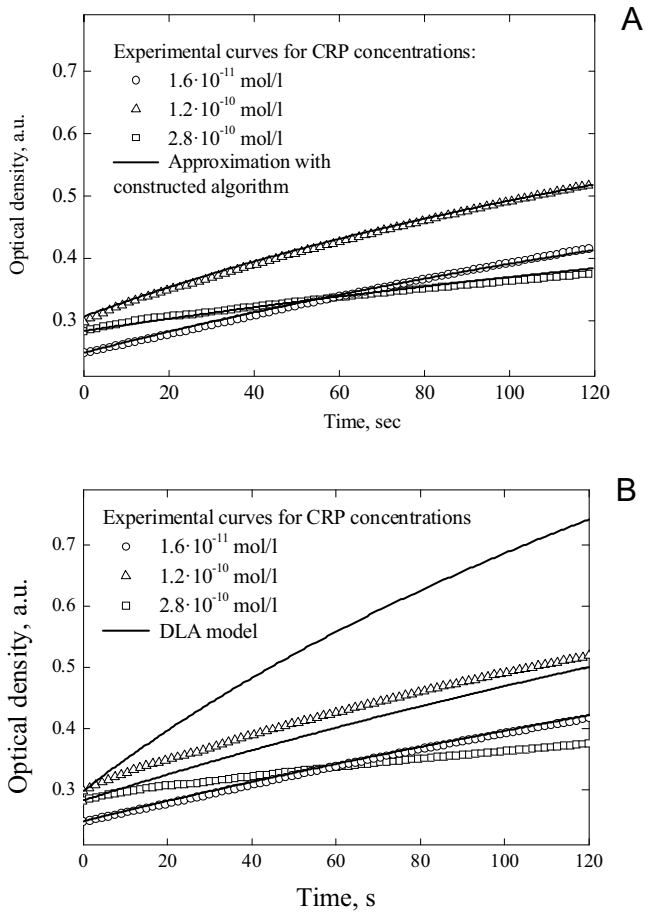

Fig. 6. Experimental OD temporal curves fitted with: A) constructed algorithm; B) standard nondiscrete DLA model with the use of determined *k11* and constant rate kernel.

Next, we simultaneously treated all 12 experimental OD curves by Eq. (22) using the DiRect [46] global optimization method varying the following parameters: K_d – the affinity of the antibody to the antigen, N – the average number of the active antibody molecules (receptors) on the single monomer particle. The values of p are then calculated for each antigen concentration using Eq. (15). The results of global optimization are presented in Fig. 6A. There is good agreement between theoretical and experimental data. As a result of fitting we obtained the target parameter values. The errors of the parameters were estimated using the Bayesian approach according

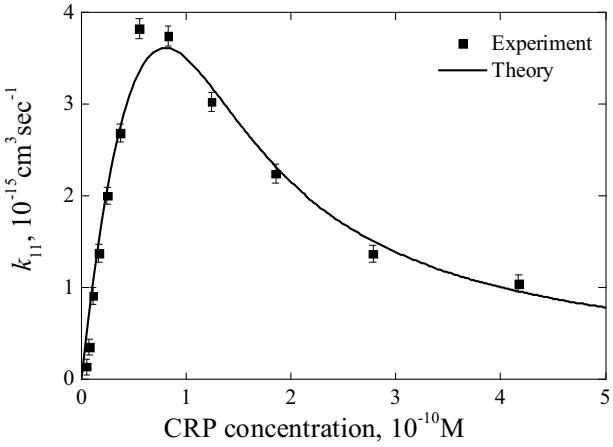

Fig. 7. The dimerization rate constant *k11* at different CRP concentrations.

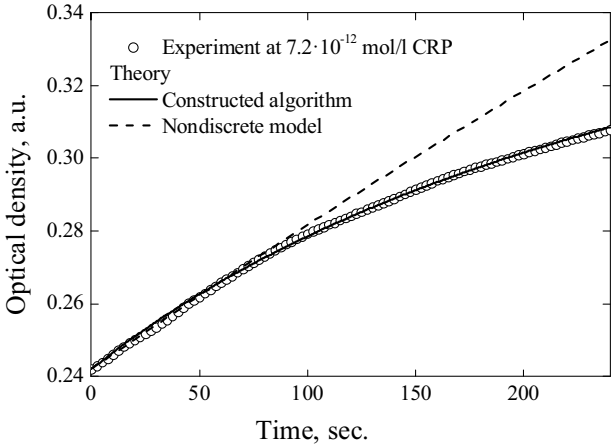

Fig. 8. The comparison of the constructed algorithm with the nondiscrete model at low antigen concentration.

to the standard methods [46]. Thus, we evaluated the target parameters of reacting agents: the average number of active antibodies on one particle N is 9.0 ± 2.2, and the affinity (inverse dissociation constant K_d) of the antigen-antibody complex is $(5.5 \pm 1.5)\,10^7\,M^{-1}$. That corresponds well to the specification of the reactants [15].

In order to compare the results of constructed optical density kinetics calculation algorithm with the standard models presented in literature we evaluated experimental values of dimerization rate constant k_{11}. If we consider only dimers formation from monomers at the initial steps of immunoagglutination process, then:

$$\frac{dC_1}{dt} = -k_{11}C_1^2, \tag{23}$$

where C_1 is the concentration of monomers. The change of the total light extinction coefficient $\Delta\alpha_{ext}$ and the dimerization rate constant k_{11} may be presented as follows:

$$\Delta\alpha_{ext} = \alpha_{ext}(t) - \alpha_{ext}(0) = C_1(t)\varepsilon_1 + C_2(t)\varepsilon_2 - C_1(0)\varepsilon_1, \tag{24}$$

$$k_{11} = \frac{\Delta\alpha_{ext}}{C_1(0)t}\frac{1}{C_1(0)(\frac{\varepsilon_2}{2} - \varepsilon_1) - \Delta\alpha_{ext}}, \tag{25}$$

With the use of Eq. (25) and of initial part of OD kinetics curve, we calculated k_{11} for all tested antigen concentrations. In this procedure the first 10 s of measured OD kinetics were used. The data obtained is presented in Fig. 7. The values represent well-known bell shaped dependence on antigen concentration. At the initial stages of immunoagglutination, when only dimers formation from monomers occurs, only k_{11} can be used according to standard La Mer model [47]. Indeed, approximation of experimental dimerization rate constants k_{11} with this model yields good results (see Fig. 7). Some discrepancies may be explained with inaccuracy in k_{11} values determination in the area of occupied antibodies prevalence, where the shifting of the reaction start point under stirring is significant. Neglecting this factor causes primarily the error in determination of the dissociation constant K_d and, in a lesser degree, of other parameters values.

An attempt of whole optical density curve reconstruction with the use of determined k_{11} values, constant kernel and computed with superposition T-matrix approach extinction cross sections of different aggregates did not give positive results (see Fig. 6B). Coincidence of theoretical calculations with experimental OD curves in most cases can be seen only in the initial region. Particularly strong differences are clearly seen for curves with low antigen concentration (Fig. 8). In these cases constant rate kernel model is unable to describe the bending of curve associated with consistent decrease in reactive particles number due to low occupation degree of discrete number of antibodies. By contrast, our model takes these effects into account and allows one to predict the behavior of agglutinating particles optical density even in the cases of small discrete number of antibodies on one particle surface.

5. Summary

Self-assembling systems of anisotropically interacting patchy particles has attracted intense attention of a large number of scientists and engineers in many interdisciplinary fields. Growing diversity and complexity of such systems requires the developing of physical properties determination methods for individual objects as well as for the whole system. This study provides understanding of diffusion-limited sterically specific aggregation kinetics in colloids. The developed method takes into account the limited number of discrete binding sites on single particles that is a key point especially for nanoparticles and/or low concentrations of the target antigen (i.e. ligand) molecules.

The method was applied for the treatment of the experimental data on the immunoagglutination kinetics registered by the turbidimetry technique. The necessity of the consideration of the limited number of discrete binding sites of single particles was demonstrated with the obtained experimental data. The developed method allows one to obtain the key parameters of the immunoagglutination system from the kinetics turbidimetric measurements, namely the ligand-receptor (antibody-antigen) affinity and the number of active receptors per particle. The study opens new perspectives in particle-enhanced immunoassay.

Acknowledgements

The experimental work was supported by Russian Foundation for Basic Research (grants 16-04-01283 and 16-34-00300), whereas Russian Science Foundation (14-15-00155) supported theoretical simulations.

References

[1] J.-M. Lehn, Toward self-organization and complex matter, Science 295 (2002) 2400–2403.
[2] L. Leibler, Nanostructured plastics: joys of self-assembling, Prog. Polym. Sci. 30 (2005) 898–914.
[3] S. Corezzi, D. Fiorettoac, F. Sciortino, Chemical and physical aggregation of small functionality particles, Soft Matter 8 (2012) 11207–11216.
[4] O. Kruglova, P.-J. Demeyer, K. Zhong, Y. Zhouac, K. Clays, Wonders of colloidal assembly, Soft Matter 9 (2013) 9072–9087.
[5] E. Bianchi, R. Blaak, C.N. Likos, Patchy colloids: state of the art and perspectives, Phys. Chem. Chem. Phys. 13 (2011) 6397–6410.

[6] W.B. Rogers, T. Sinno, J.C. Crocker, Kinetics and non-exponential binding of DNA-coated colloids, Soft Matter 9 (2013) 6412–6417.
[7] F. Sciortino, C. Michele, S. Corezzi, J. Russo, E. Zaccarelli, P. Tartaglia, A parameter-free description of the kinetics of formation of loop-less branched structures and gels, Soft Matter 5 (2009) 2571–2575.
[8] S. Xu, Z. Sun, Progress in coagulation rate measurements of colloidal dispersions, Soft Matter 7 (2011) 11298–11308.
[9] Z. Sun, J. Liu, S. Xu, Study on improving the turbidity measurement of the absolute coagulation constant, Langmuir 22 (2006) 4946–4951.
[10] A.M. Puertas, F.J. Nieves, A new method for calculating kinetic constants within the Rayleigh – Gans – Debye approximation from turbidity measurements, J Phys Condens Matter 9 (1997) 3313–3320.
[11] S. Xu, Z. Sun, Evaluation of the uncertainties caused by the forward scattering in turbidity measurement of the coagulation rate, Langmuir 26 (2010) 6908–6918.
[12] L. Gmachowski, M. Paczuski, Fractal dimension of asphaltene aggregates determined by turbidity, Colloid Surface A 384 (2011) 461–465.
[13] A. Torcello-Gomez, M.J. Santander-Ortega, J.M. Peula-Garcıa, J. Maldonado-Valderrama, M.J. Galvez-Ruiz, J.L. Ortega-Vinuesa, A. Martın-Rodrıguez, Adsorption of antibody onto Pluronic F68-covered nanoparticles: link with surface properties, Soft Matter 7 (2011) 8450–8461.
[14] E.V. Piletska, S.A. Piletsky, Size matters: influence of the size of nanoparticles on their interactions with ligands immobilized on the solid surface, Langmuir 26 (2010) 3783–3785.
[15] J.A. Molina-Bolvar, F. Galisteo-Gonzalez, R. Hidalgo-Alvarez, Fractal aggregates induced by antigen-antibody interaction, Langmuir 17 (2001) 2514–2520.
[16] H. Colfen, A. Volkel, S. Eda, U. Kobold, J. Kaufmann, A. Puhlmann, C. Goltner, H. Wachernig, Mechanism of nanoparticle-enhanced turbidimetric assays applying nanoparticles of different size and immunoreactivity, Langmuir 18 (2002) 7623–7628.
[17] J.A. Molina-Bolivar, F. Galisteo-Gonzalez, Latex immunoagglutination assays, J. Macromol. Sci. C 45 (2005) 59–98.
[18] S. Stone, G. Bushell, R. Amal, Z. Ma, H.G. Merkus, B. Scarlett, Characterization of large fractal aggregates by small-angle light scattering, Meas. Sci. Technol. 13 (2002) 357–364.
[19] J.W. Virden, J.C. Berg, The use of photon correlation spectroscopy for estimating the rate constant for doublet formation in an aggregating colloidal dispersion, J. Colloid Interface Sci. 149 (1992) 528–535.
[20] S. Xu, J. Liu, Z. Sun, Optical factors determined by the T-matrix method in turbidity measurement of absolute coagulation rate constants, J. Colloid Interface Sci. 304 (2006) 107–114.
[21] A. Fernandez-Barbero, M. Cabrerizo, R. Martinez, R. Hidalgo-Alvarez, Coagulation of polymer colloids by IgG molecules, Prog. Colloid Polym. Sci. 93 (1993) 269–272.
[22] M.A. Yurkin, A.G. Hoekstra, The discrete-dipole-approximation code ADDA: capabilities and known limitations, J. Quant. Spectrosc. Radiat. Transfer 112 (2011) 2234–2247.
[23] O. Merchiers, C. Eyraud, J.-M. Geffrin, R. Vaillon, B. Stout, P. Sabouroux, B. Lacroix, Microwave measurements of the full amplitude scattering matrix of a complex aggregate: a database for the assessment of light scattering codes, Opt. Express 18 (2010) 2056–2075.
[24] M. Quesada, J. Puig, J.M. Delgado, J.M. Peula, J.A. Molina, R. Hidalgo-Alvarez, A simple kinetic model of antigen-antibody reactions in particle-enhanced light scattering immunoassays, Colloid Surface B 8 (1997) 303–309.
[25] M.C. Heine, S.E. Pratsinis, Brownian coagulation at high concentration, Langmuir 23 (2007) 9882–9890.
[26] E. Pefferkorn, R. Varoqui, Dynamics of latex aggregation. Modes of cluster growth, J. Chem. Phys. 91 (1989) 5679–5686.
[27] T.A. Witten, L.M. Sander, Diffusion-limited aggregation, Phys. Rev. B 27 (1983) 5686–5697.
[28] A. Moncho-Jorda, G. Odriozola, M. Tirado-Miranda, A. Schmitt, R. Hidalgo-Alvarez, Modeling the aggregation of partially covered particles: theory and simulation, Phys. Rev. E 68 (2003) 011404.
[29] A. Giacometti, F. Lado, J. Largo, G. Pastore, F. Sciortino, Effects of patch size and number within a simple model of patchy colloids, J. Chem. Phys. 132 (2010) 174110.
[30] R.C. Ball, D.A. Weitz, T.A. Witten, F. Leyvraz, Universal kinetics in reaction-limited aggregation, Phys. Rev. Lett. 58 (1987) 274–277.
[31] V.M. Berdnikov, A.B. Doktorov, Steric factor in diffusion-controlled chemical reactions, Chem. Phys. 69 (1982) 205–212.
[32] C.J. van Oss, Precipitation and agglutination, J. Immunoassay 21 (2000) 143–164.
[33] M.L. Broide, R.J. Cohen, Measurements of cluster-size distributions arising in salt-induced aggregation of polystyrene microspheres, J. Colloid Interface Sci. 153 (1992) 493–508.
[34] I.V. Surovtsev, M.A. Yurkin, A.N. Shvalov, V.M. Nekrasov, G.F. Sivolobova, A.A. Grazhdantseva, V.P. Maltsev, A.V. Chernyshev, Kinetics of the initial stage of immunoagglutionation studied with the scanning flow cytometer, Colloid Surface B 32 (2003) 245–255.
[35] M. Wiklund, O. Nord, R. Gothall, A.V. Chernyshev, P.A. Nygren, H.M. Hertz, Fluorescence-microscopy-based image analysis for analyte-dependent particle doublet detection in a single-step immunoagglutination assay, Anal. Biochem. 338 (2005) 90–101.
[36] V.M. Nekrasov, A.A. Polshchitsin, M.A. Yurkin, G.E. Yakovleva, V.P. Maltsev, A.V. Chernyshev, Brownian aggregation rate of colloid particles with several active sites, J. Chem. Phys. 141 (2014) 064309.
[37] D.W. Mackowski, Electrostatics analysis of radiative absorption by sphere clusters in the Rayleigh limit: application to soot particles, Appl. Opt. 34 (1995) 3535–3545.
[38] M.I. Mishchenko, L.D. Travis, D.W. Mackowski, T-matrix computations of light scattering by nonspherical particles: a review, J. Quant. Spectrosc. Radiat. Transfer 55 (1996) 535–575.
[39] M. Tirado-Miranda, A. Schmitt, J. Callejas-Fernandez, A. Fernandez-Barbero, Dynamic scaling and fractal structure of small colloidal clusters, Colloid Surface A 162 (2000) 67–73.
[40] Z. Yang, H. Yang, Z. Jiang, X. Huang, H. Li, A. Li, R. Cheng, A new method for calculation of flocculation kinetics combining Smoluchowski model with fractal theory, Colloid Surface A 423 (2013) 11–19.
[41] D.T. Gillespie, A general method for numerically simulating the stochastic time evolution of coupled chemical reactions, J. Comp. Phys. 22 (1976) 403–434.
[42] M.I. Mishchenko, J.M. Dlugach, Radar polarimetry of Saturn's rings: modeling ring particles as fractal aggregates built of small ice monomers, J. Quant. Spectrosc. Radiat. Transfer 110 (2009) 1706–1712.
[43] M. Kobayashi, D. Ishibashi, Absolute rate of turbulent coagulation from turbidity measurement, Colloid Polym. Sci. 289 (2011) 831–836.
[44] J.A.J. Baker, P. Graves-Morris, Pade Approximants, Cambridge University Press, New York, 1996.
[45] F. Calogero, F. Leyvraz, A new solvable model of aggregation kinetics, J. Phys. A: Math. Gen. 32 (1999) 7697–7717.
[46] D.I. Strokotov, M.A. Yurkin, K.V. Gilev, D.R. Bockstaele, A.G. Hoekstra, N.B. Rubtsov, V.P. Maltsev, Is there a difference between T- and B-lymphocyte morphology? J. Biomed. Opt. 14 (2009) 064012–064036.
[47] R.H. Smellie, V.K. La Mer, Flocculation, subsidence and filtration of phosphate slimes: VI. A quantitative theory of filtration of flocculated suspensions, J. Colloid Sci. 13 (1958) 589–599.